

University of Warwick institutional repository: <http://go.warwick.ac.uk/wrap>

This paper is made available online in accordance with publisher policies. Please scroll down to view the document itself. Please refer to the repository record for this item and our policy information available from the repository home page for further information.

To see the final version of this paper please visit the publisher's website. Access to the published version may require a subscription.

Author(s): G. Nisbet, C.L.A. Lamont, M. Polcik, R. Terborg, D.I. Sayago, J.T. Hoefl, M. Kittel, R.L. Toomes and D.P. Woodruff
Article Title: Structural analysis of Pt(1 1 1)c($\sqrt{3} \times 5$)rect.-CO using photoelectron diffraction

Year of publication: 2007

Link to published version:

<http://dx.doi.org/10.1016/j.susc.2006.12.073>

Publisher statement: Nisbet, G. et al. (2007). Structural analysis of Pt(1 1 1)c($\sqrt{3} \times 5$)rect.-CO using photoelectron diffraction. Surface Science, Vol. 601, pp. 1296-1303

Structural analysis of Pt(111)-c($\sqrt{3} \times 5$)rect-CO using photoelectron diffraction

G. Nisbet¹, C.L.A. Lamont^{1*}, M. Polcik², R. Terborg², D.I. Sayago², J.T. Hoeft², M. Kittel², R.L. Toomes³ and D.P. Woodruff³,

¹ Dept. of Chemical & Biological Sciences, University of Huddersfield, Queensgate, Huddersfield HD1 3DH, UK

² Fritz-Haber-Institut der Max-Planck-Gesellschaft, Faradayweg 4-6, 14195 Berlin, Germany

³ Physics Dept, University of Warwick, Coventry CV4 7AL, UK

Abstract

Core level shift scanned-energy mode photoelectron diffraction using the two distinct components of the C 1s emission has been used to determine the structure of the Pt(111)c($\sqrt{3} \times 5$)rect.-CO phase formed by 0.6 ML of adsorbed CO. The results confirm earlier assignments of these components to CO in atop and bridging sites, further confirm that the best structural model involves a 2:1 occupation ratio of these two sites, and provides quantitative structural parameter values. In particular the Pt-C chemisorption bondlengths for the atop and bridging sites are, respectively, 1.86 ± 0.02 Å and 2.02 ± 0.04 Å. These values are closely similar to those found in the 0.5 ML coverage c(4x2) phase, involving an atop:bridge occupation ratio of 1:1, obtained in earlier quantitative low energy electron diffraction studies. The results also indicate a clear tilt of the molecular axis of atop CO species in this compression phase, consistent with the finding of an earlier electron-stimulated desorption ion angular distribution investigation.

Keywords: Carbon monoxide; Photoelectron diffraction; Platinum; Surface structure

1. Introduction

The interaction of CO with Pt surfaces is one of the most studied problems in surface science, in part as a ‘simple’ model system of chemisorption, and in part because of the relevance of the system to CO oxidation catalysis. The structural aspects of CO adsorption on transition metals in general is surprisingly complex, indicating subtle variations with material, crystal face and coverage. Typically CO occupies either atop (one-fold coordinated), bridge (two-fold coordinated) or hollow (three-fold or four-fold coordinated) adsorption sites, but the preferred site at low coverage differs on different surfaces and may change with increasing coverage. Early qualitative LEED (low energy electron diffraction) observations of CO adsorption on Pt(111) show a whole sequence of different ordered phases with increasing coverage [1], with the higher coverage phases showing apparent continuous variation in unit mesh dimensions consistent with a uniaxial compression of the overlayer. Initially, such LEED patterns in other systems were interpreted in terms of a ‘floating’ overlayer which at intermediate coverages was incommensurate with the substrate [2] (implying an infinite variety of local adsorption sites). This picture, however, was revised largely as a consequence of the interpretation of the results of vibrational spectroscopic studies using electron energy loss spectroscopy (EELS) and reflection-absorption infra-red spectroscopy (RAIRS).

The approximate value of the C-O stretching frequency provides a basis for identifying the probable bonding coordination, based on the large body of data on carbonyl compounds (e.g. [3]). Both EELS [4, 5, 6, 7] and RAIRS [8, 9, 10] measurements for CO on Pt(111) showed that for coverages up to the nominal 0.33 ML of the ordered $(\sqrt{3}\times\sqrt{3})R30^\circ$ phase the spectra indicate pure atop site adsorption, whereas at higher coverages a mixture of atop and bridge sites are occupied. The fact that these vibrational data indicate only occupation of (approximately) high-symmetry sites led to a revised picture of the compression phases as all being locally commensurate with the intermediate average mesh sizes inferred from the LEED patterns being due to moving inter-domain boundary walls [11, 12, 13]. Fig. 1 illustrates this, showing models of the 0.5 ML $c(4\times 2)$ phase (which may also be described as $(\sqrt{3}\times 2)\text{rect.}$), the 0.6 ML

$c(\sqrt{3}\times 5)\text{rect.}$, and the 0.67 ML $c(\sqrt{3}\times 3)\text{rect.}$ phases as proposed by Persson *et al.* [13]. In going from 0.5 ML to 0.6 ML the number of atop CO molecules has been increased to produce the zig-zag row of atop species in the $c(\sqrt{3}\times 5)\text{rect.}$ phase, and the spacing of these dense zig-zag rows then decreases with increasing coverage. By increasing the density of atop species in these rows, and varying their spacing, a large sequence of different structural phases can be formed, and fluctuations in the spacing of these atop chains can lead to intermediate average periodicities as sampled by the LEED pattern. Notice that the near-neighbour occupation of the atop sites in the dense rows may be expected to lead to a tilt of the C-O axes for these molecules due to intermolecular repulsion, as shown schematically in fig. 1.

Here we should note that adsorption site identification on the basis of vibrational spectroscopy has not always proved to be consistent with true quantitative structural methods; in particular, 0.5 ML $c(4\times 2)$ phases of CO on both Ni(111) and Pd(111) were widely believed to involve pure bridge site occupation on the basis of the measured value of the C-O stretching frequency, whereas subsequent structure determinations for Ni(111) using PhD (scanned-energy mode photoelectron diffraction) [14, 15] and quantitative LEED [16], and for Pd(111) using PhD [17], have shown that the true structure in both cases involves only three-fold coordinate hollow site occupation. For Pt(111)/CO, however, the two distinct vibrational absorption bands at frequencies entirely consistent with the atop and bridge assignments seems far less open to doubt, but even more importantly, quantitative LEED structure determinations [18,19] of the 0.5 ML $c(4\times 2)$ phase in this case have provided clear confirmation of the structure shown in fig. 1 in which 0.25 ML of CO molecules occupy atop sites while a further 0.25 ML CO occupy bridge sites. A detailed STM (scanning tunnelling microscopy) investigation of this phase that also included full theoretical modelling of the images also clearly favoured this structural model for the $c(4\times 2)$ phase over alternative models based on other mixtures of atop, hollow and bridge sites [20].

While vibrational spectroscopies provide a clear spectral fingerprint of the local atop and bridge adsorption sites, and show that some mixture of these sites is occupied in all the

higher coverage ‘compression’ phases, they do not provide a secure basis for determining the relative occupation of these two sites at different coverages. This is because the relative intensities of the absorption bands can be influenced by a range of vibrational coupling effects in addition to the number of contributing molecules. Core level (X-ray) photoelectron spectroscopy (XPS), on the other hand, does show a clear linear relationship between photoemission intensity and coverage, and both C 1s and O 1s XPS signals from CO on Pt(111) show clear ‘chemical’ shifts in the photoelectron binding energies between emission from molecules in the atop and bridge sites. These spectra show clearly that the $c(4 \times 2)$ phase does correspond to equal occupation of the two distinct local sites, while at higher coverages an increasing fraction of atop sites are occupied [21].

The Pt(111)/CO system has also been subjected to many theoretical studies, including several using what are generally regarded as the most sophisticated and reliable methodologies in density functional theory (DFT) slab calculations. However, these calculations have revealed a systematic failure to correctly determine the energetically-preferred adsorption site at low coverage, such calculations consistently favouring hollow sites rather than the atop site seen in experiments [22]. Several recent publications have explored the origins of this effect and claimed to overcome this problem (e.g. [23, 24, 25, 26, 27]), but there seems to be no general acceptance of a satisfactory solution. In view of this it is unclear whether such methods yield meaningful results for the more complex Pt(111)/CO structural phases at high coverages, although calculations constrained to the experimentally-determined adsorption sites may be expected to still give the correct optimised geometry for these sites. There appears to be one such calculation for the $c(4 \times 2)$ phase [28].

The XPS core level shifts (CLS) mentioned above also provide a route to a more incisive local structure determination of these mixed-site surface phases using photoelectron diffraction. In this technique [29] one exploits the coherent interference between the directly-emitted component of the photoelectron wavefield ejected from an adsorbate atom core level, and components of the same wavefield elastically scattered by the

surrounding atoms. This interference leads to modulations in the detected intensity as a function of the direction or photoelectron energy (and thus photoelectron wavelength), due to changes in the relative phase of different scattering paths. By working at relatively low photoelectron energies (~ 100 - 400 eV), backscattering from the substrate atoms is strong and dominates the detected diffraction modulations. The technique provides *local* structural information about the (adsorbate) emitter atom that is intrinsically element-specific, but also chemical-state specific through changes in the photoelectron binding energy. In the Pt(111)/CO case it is therefore possible to obtain essentially independent local structural information on the bridge and atop CO species by measuring the photoelectron diffraction from each CLS component of the C 1s or O 1s photoemission. In this respect the method is significantly more incisive than the ‘benchmark’ surface structural technique of quantitative LEED. In fact, this chemical-state-specificity of photoelectron diffraction has already been exploited by Bondino *et al.* [30] using measurements of the polar and azimuthal angle dependence of the C 1s emission to provide an independent determination of the local structure of the $c(4 \times 2)$ phase. Notice that this study also provided positive identification of the origin of the two C 1s components that had previously relied only on spectral fingerprinting. The results of the CLS photoelectron diffraction study are in generally good agreement with those of the quantitative LEED studies, although there do appear to be slight but significant differences in the structural parameters (notably the Pt-CO bondlengths) obtained.

Here we present the results of a structure determination of the $c(\sqrt{3} \times 5)$ rect. phase of CO on Pt(111) obtained at a nominal coverage of 0.6 ML using the alternative scanned energy mode form of photoelectron diffraction, but also exploiting the C 1s CLS between the atop and bridging species. We have used this PhD technique in the past to solve a large range of adsorption structures (e.g. [29]) (including the $c(4 \times 2)$ phases of CO on Ni(111) and Pd(111) mentioned above), and by using a substantial data base of PhD spectra are able to achieve rather complete and precise local structure determinations. In the present case our primary aim is to gain detailed quantitative structural information on the local geometries of the two species, and to compare these with those found in the $c(4 \times 2)$ phase by LEED and angle-scan photoelectron diffraction. We also wish to provide

an independent test of the proposal, based on ESDIAD (electron-stimulated desorption ion angular distribution) data [31], and favoured by various theoretical treatments (e.g. [13, 32]), that the higher coverage (>0.5 ML) phase involves tilting of the C-O axes away from the surface normal. In addition, we seek to distinguish different models that have been proposed of the long-range ordering of the atop and bridge species in the $c(\sqrt{3}\times 5)$ rect. unit mesh. While the PhD technique is primarily sensitive to the *local* structure, scattering by near-neighbour adsorbates can provide some sensitivity to the long-range ordering model.

2. Experimental Details

The experiments were performed in an ultra-high vacuum surface science end-station operating at a base pressure of 10^{-10} mbar and equipped with typical facilities for sample cleaning, heating and cooling. This instrument was installed on from the UE56/2-PGM1 beamline [33] at the BESSY II synchrotron radiation facility in Berlin. Different electron emission directions can be detected (using an Omicron EA-125HR 125 mm mean radius hemispherical electrostatic analyser, equipped with seven-channeltron parallel detection), by rotating the sample about its surface normal (to change the azimuthal angle) and about a vertical axis (to change the polar angle). The Pt(111) crystal was cleaned in situ by cycles of Ar ion sputtering and annealing at 640°C , until a well-ordered (1x1) surface free from impurities was obtained as judged by LEED and (synchrotron radiation) XPS. CO dosing was performed at a sample temperature of 160 K, and the formation of a $c(\sqrt{3}\times 5)$ rect. overlayer phase was confirmed by LEED. As shown in fig. 2, the C 1s photoemission spectrum, shown here measured at a photon energy of 495 eV, clearly shows the presence of two component peaks, separated by an energy of ~ 0.70 eV. The peak at lower kinetic energy, believed to be associated with the atop CO, shows a far more pronounced low kinetic energy shoulder than that of the higher energy peak; this effect has also been noted in previous studies [21, 30], although in the present case the shoulder seems to be more distinctly resolved. Note that the small feature at a kinetic energy some 2 eV higher than the bridging CO is probably due to a small coverage of atomic C.

C 1s PhD spectra were recorded in the photoelectron kinetic energy range of 68 - 372 eV, at 3 eV intervals in photon energy, at polar emission angles between 0° and 60° from the surface normal in the $[\bar{1}10]$, $[\bar{1}\bar{2}\bar{1}]$ and $[\bar{2}\bar{1}1]$ azimuths. At each step in the photon energy an energy distribution curve (EDC) around the C 1s peak was recorded covering a kinetic energy window of 28 eV. The analyser pass energy and step size were chosen such that the two C 1s peaks could be clearly resolved, while also giving a satisfactory signal-to-noise ratio. It should be noted that although Pt Auger peaks are present in the background over the chosen energy range, the fact that they are much broader than the C 1s peaks means that so long as each EDC has been measured over a suitably wide energy window, the normalisation procedures which are applied in the analysis allow the contribution of these Auger peaks to be separated from the photoemission peaks. To extract the PhD modulation spectra, each EDC was first fitted by a sum of two Gaussian peaks and two associated background steps. The integrated area of each component peak was then plotted as a function of kinetic energy, $I(E)$. A stiff spline function, $I_0(E)$, through these data was then subtracted and the resulting function was divided by the spline function, to yield the PhD modulation spectrum $\chi(E)=(I(E)-I_0E)/I_0(E)$. Notice that the presence of the shoulder on the lower kinetic energy C 1s peak meant that this component was relatively poorly described by a Gaussian peak. Additional fits were therefore tested using three component peaks, the third component fitting this shoulder. The resulting PhD spectra showed that the shoulder displayed the modulations of the main low energy peak and these were quite different from those of the higher energy peak. This clearly confirms that the shoulder is associated with the same emitter atoms as the main low energy peak. These tests also indicated that the PhD spectra for the lower energy peak were largely independent of the method of peak fitting used.

3. Results and structure determination

A subset of the experimental C 1s PhD spectra in different emission directions (fig. 3), 6 from the lower kinetic energy (atop) component, 5 from the higher energy (bridge) component, was then used as the basis for the structure determination. The spectra were

selected to provide a reasonable range of emission directions, but also focussed on those showing the largest modulation amplitudes. It is the spectra with the largest amplitudes that are expected to be most accurately represented by the multiple scattering simulations, and typically these correspond to emission directions that place a substrate scatterer atom almost directly behind the emitter relative to the detector, giving the favoured 180° scattering geometry. For this reason we expect the largest modulations to occur in different emission directions for the atop and bridge species, and indeed it is notable that the PhD spectra from the low energy peak show the strongest near-single-period modulations at normal emission, consistent with an atop site, while those from the higher energy peak show the strongest modulations at an emission angle of $\sim 30\text{-}40^\circ$ in the $[\bar{1}10]$ azimuth, consistent with a bridge-site emitter. In general, however, all the modulations are rather weak, typically being only $\sim \pm 10\%$ even in these directions. More typically, in PhD, one may obtain modulations of $\sim \pm 40\%$ or more for high-symmetry adsorption sites. The reason for these weak modulations is attributable to the special scattering characteristics of Pt atoms that show a broad minimum in the backscattering cross-section in the energy range relevant to these measurements. This same effect is well-known in EXAFS and leads to similar problems of unusually weak modulations.

In order to extract the structure from these measurements, multiple scattering curved-wave calculations must be performed for a range of trial structures, using a computer code developed by Fritzsche [34, 35]. This theoretical formulation is based on a magnetic quantum number expansion and takes into account the finite acceptance angle of the detector (5°) and the energy resolution of the experiment (5eV). These factors help to reduce the importance of longer scattering pathways, and ensure that fourth and higher order scattering events can largely be ignored. To quantify the agreement between the theoretical and experimental modulation functions a reliability factor, R_m is calculated using the equation:

$$R_m = \frac{\sum_{i=1}^m (\chi_{th}^i - \chi_{exp}^i)^2}{\sum_{i=1}^m (\chi_{th}^{i^2} + \chi_{exp}^{i^2})}$$

χ_{exp} is the experimental modulation curve, while χ_{th} is the theoretical modulation curve. R_m is the normalised sum of the squares of the differences between χ_{exp} and χ_{th} and should be as close to zero as possible. Typically, in a range of structural studies using this approach, values in the range $\sim 0.1-0.3$ have been found to be achievable, although the weak modulations found in the present system might lead us to expect the best fits here to be in the upper end of this range.

The first stage of the structure determination was to establish the approximate local site of each of the two C emitters. In particular, we wished to establish independently the coordination site associated with the two chemically-shifted components. Model calculations were therefore performed for all four high-symmetry adsorption sites, namely atop, bridge and the two symmetrically distinct three-fold coordinated hollow sites referred to as the fcc site (directly above a third layer Pt atom) and the hcp site (directly above a second layer Pt atom). In each site the primary structural parameters, namely the C-Pt layer spacing and the C-O bondlength, were adjusted to minimise the R -factor. However, all of these calculations assumed a bulk-terminated Pt(111) substrate and a C-O axis perpendicular to the surface. The objective of these calculations is to obtain the approximate local site only, and not to investigate the possible role of intermolecular scattering in different specific models. For simplicity the calculations were based on the distribution of CO molecules found in the well-established $c(4 \times 2)$ phase, which contains no very short CO-CO distances and thus only a weak contribution from intramolecular scattering. The best R -factor values for each site and for each component C 1s peak are summarised in Table 1. Clearly much the lowest R -factor for each C 1s component corresponds to the expected location, namely atop for the low kinetic energy component and bridge for the high kinetic energy component. To assess the significance of this, however, we may calculate the variance in the two minimum R -

factor values, defined as $\text{var}(R_{\min}) = R_{\min} \sqrt{(2/N)}$, where N is a measure of the number of independent pieces of information in the experimental data defined and discussed elsewhere [36]. For the low kinetic energy component the resulting variance is 0.058, while for the high energy component it is 0.056. We may reject any solution that has an *R*-factor value greater than $R_{\min} + \text{var}(R_{\min})$, which, as may be seen from Table 1, clearly excludes any of the other adsorption sites.

A second stage of structural refinement was then undertaken in which relaxation of individual atoms in the outermost Pt layer perpendicular to the surface, and tilting of the C-O axis relative to the surface normal (in the azimuth found in the ESDIAD experimental study). In addition, three different models of the possible ordering of the atop and bridge CO species, shown in fig. 4, were considered. (a) is the model proposed by Persson *et al.* [13] as shown in fig. 1, while (b) is the model suggested by Avery in an early EELS publication [6], which shows denser atop chains and more widely-spacing CO molecules in bridging sites. Notice, though, that model (b) strictly has $(\sqrt{3} \times 5)\text{rect.}$ periodicity, and not $c(\sqrt{3} \times 5)\text{rect.}$, so this structure should lead to additional LEED beams not reported in the experiments; it is possible, however, that these additional beams may be weak. Model (c) in fig. 4, is quite different, and was proposed by Petrova and Yakovkin [37] on the basis of a reassessment of the published LEED patterns and kinematical theory (single scattering) modelling of these patterns. In truth it is far from clear that the basis of this analysis is sound; certainly this paper contains misleading information regarding ‘missing’ diffracted beams for the accepted structure of the Ni(111) $c(4 \times 2)$ -CO phase which is an artefact of the kinematic simplification. However, a key feature of the model of fig. 4(c) is that it contains twice as many bridge CO as atop CO molecules, whereas this atop:bridge ratio is reversed for models (a) and (b). As has been mentioned in the introduction, the previously-published XPS data of Bjorneholm *et al.* [21] clearly shows that this third model cannot be correct; XPS shows the atop:bridge occupation ratio is 2:1, not 1:2, and our own confirmation that the low and high kinetic energy peaks do correspond to the atop and bridge sites reinforces this interpretation. Our own photoemission spectra add further confirmation. Because of the modulation effect of photoelectron diffraction at the lower kinetic energies of our measurements a comparison

of the component intensities of individual EDCs will not provide a reliable measure of the relative occupation, but an average of many such measurements will. We also find an atop:bridge ratio of approximately 2.

Distinguishing models (a) and (b) of fig. 4 is more difficult using PhD, because the main difference is the number of atop neighbours (all of the same separation) in the atop chains, and the extent to which the bridge CO molecules do, or do not, have atop CO molecules as near neighbours. The two models also differ in the number of CO molecules expected to tilt, but the magnitude of the tilt angles is unknown in both models. In fact the optimisation of the structures of these two models does lead to slightly lower R -factor values for model (a) to model (b). The global R -factors (summing over both the atop and bridge PhD spectra) are 0.24 and 0.26 respectively, but with a variance in the minimum of 0.03 this difference is not formally significant. However, for the bridge site PhD spectra alone the R -factors for the (a) and (b) models are 0.25 and 0.31 respectively, with a variance in R_{\min} of 0.05, rendering the difference just significant. The R -factor for the atop C 1s PhD spectra is also lower (0.19) for model (a) than for model (b) (0.22) although in this case this difference falls just within the variance. Bearing in mind that we may expect the bridge site CO emitters to be more sensitive to the difference in these models (with or without atop CO neighbours) we therefore conclude that model (a) is the preferred structure. Of course, the fact that the two LEED patterns should be different is also a further factor, beyond the PhD analysis, which favours model (a).

The structural parameter values found for this best-fit structural model are summarised in Table 2, where they are compared with similar parameters for the c(4x2) phase from the LEED and angle-scan photoelectron diffraction studies. In general the structural parameter values found in our study are all in excellent agreement with the LEED parameters for the c(4x2) phase; in this regard the Pt-CO bondlengths found in the angle-scan photoelectron diffraction study of this phase do appear to be systematically slightly larger. Our optimised structure also shows clear evidence for a tilt of the atop CO molecules; for the bridging CO molecules the precision is too low to draw any clear conclusions, but the results are clearly consistent with the expected perpendicular orientation of these species as shown in fig. 4(a). ESDIAD of CO⁺ desorption clearly

shows a tilt angle of 6° , and the desorption of this species is believed to be dominated by the contribution from the atop species; the ESDIAD data thus provide no information on any possible tilt of the bridging CO species. Table 2 also shows that the structural parameters obtained in the DFT calculations for the $c(4 \times 2)$ structure and, for the atop CO tilt angle, for a hypothetical $(\sqrt{3} \times 3)$ structure. Clearly the bond lengths found in these DFT calculations agree well with the LEED data and our results, consistent with the notion that the failure in DFT for this system is in determining the relative energy of the atop and hollow sites, but not the associated optimised geometries.

4. Conclusions

Our CLS PhD investigation of the structure of the $\text{Pt}(111)c(\sqrt{3} \times 5)\text{rect.}-\text{CO}$ phase formed by 0.6 ML of adsorbed CO provides clear support for the mixed atop + bridging site model, based on a 2:1 occupation ratio, previously proposed on the basis of the observed LEED patterns and vibrational spectroscopic data [13]. It also provides clear support for the previously assumed assignment of the chemically-shifted components of the C 1s photoemission spectrum. Consideration of three alternative models of the arrangement of the atop and bridge CO molecules within the unit mesh leads to a clear preference for the model mentioned above, in part based on the PhD data. The local structural parameters, notable the Pt-C chemisorption bond lengths found in this analysis are entirely consistent with the values obtained in LEED studies of the 0.5 ML $c(2 \times 4)$ phase, but highlight a slight numerical discrepancy of these two sets of results with an earlier CLS photoelectron diffraction study of the $c(4 \times 2)$ phase based on angle-scan data. The PhD results also indicate a clear tilt of the atop CO molecular axes in this compression phase, consistent with the finding of an earlier ESDIAD investigation.

Acknowledgements

The authors acknowledge the financial support of the Physical Sciences and Engineering Research Council (UK).

Table 1

Summary of lowest R -factor values found in the first-order structure analysis for each of the different possible high-symmetry local adsorption sites for the PhD spectra from the two C 1s chemically-shifted components

Adsorption site	low KE peak	high KE peak
	R -factor	R -factor
atop	0.31	0.78
bridge	0.78	0.27
Fcc hollow	0.65	0.90
Hcp hollow	0.92	0.65

Table 2

Summary of structural parameter values for the best-fit structure (fig. 4(a)) found in this CLS PhD study of the Pt(111) $c(\sqrt{3}\times 5)$ rect.-CO phase compared with values for the LEED and angle-scan photoelectron diffraction (AS-PD) investigations of the Pt(111) $c(4\times 2)$ -CO phase and the tilt angle found for the high coverage phases in ESDIAD. $\Delta z(a)$ is the outward relaxation of the outermost Pt atoms labelled a (directly below the atop CO) in fig. 4(a), $\Delta z(b)$ is the same parameter for the b atoms of this fig (Pt atoms bonding to the bridging CO) and $\Delta z(c)$ is the same parameter for the c atoms of this fig (Pt atoms not bonded to CO)

	this work <i>c</i> ($\sqrt{3}\times 5$) <i>rect</i>	LEED <i>c</i> (4x2)	AS-PD [30] <i>c</i> (4x2)	DFT [28] <i>c</i> (4x2)	ESDIAD [31] <i>c</i> ($\sqrt{3}\times 5$) <i>rect</i>
$d_{\text{Pt-C(atop)}} \text{ \AA}$	1.86 ± 0.02	1.85 ± 0.10 [18] 1.91 ± 0.04 [19]	1.98 ± 0.04	1.87	-
$d_{\text{Pt-C(bridge)}} \text{ \AA}$	2.02 ± 0.04	2.08 ± 0.07 [18] 1.97 ± 0.04 [19]	2.13 ± 0.04	2.02	-
$d_{\text{C-O(atop)}} \text{ \AA}$	1.24 ± 0.05	1.15 ± 0.05 [18] 1.12 ± 0.04 [19]	fixed	1.15	-
$d_{\text{C-O(bridge)}} \text{ \AA}$	1.25 ± 0.15	1.15 ± 0.05 [18] 1.19 ± 0.04 [19]	fixed	1.19	-
C-O tilt atop $^{\circ}$	11 ± 3	-	-	13	6
C-O tilt bridge $^{\circ}$	8 (+13/-30)	-	-	-	-
$\Delta z(a) \text{ \AA}$	+0.02	$+0.02 \pm 0.04$ [19]	-	-	-
$\Delta z(b) \text{ \AA}$	+0.01	$+0.02 \pm 0.04$ [19]	-	-	-
$\Delta z(c) \text{ \AA}$	-0.05	-0.05 ± 0.04 [19]	-	-	-
R-factor	0.24	-	-	-	-

Figure Captions

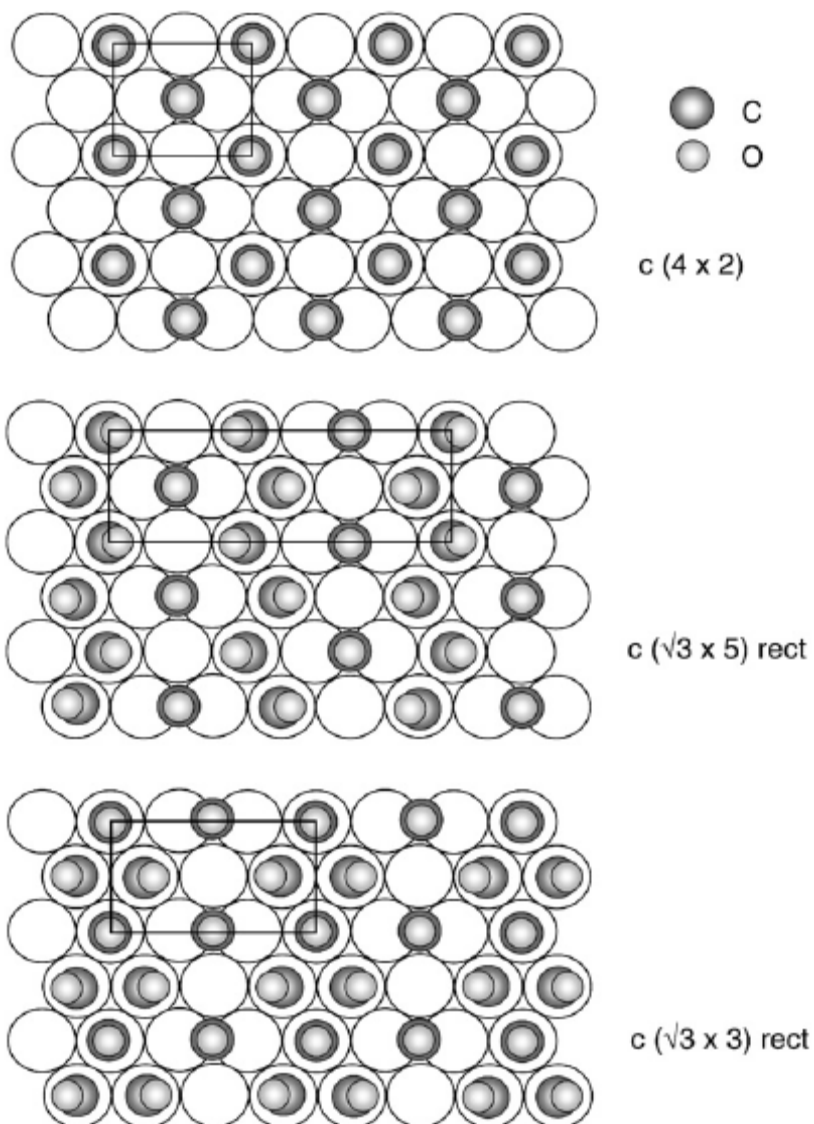


Fig. 1 Schematic diagram of the $c(4 \times 2)$ (which may also be described as $(\sqrt{3} \times 2)$ rect.), $c(\sqrt{3} \times 5)$ rect. and $c(\sqrt{3} \times 3)$ rect. phases for CO on Pt(111) at nominal coverages of 0.50 ML, 0.60 ML and 0.67 ML, as proposed by Persson *et al.* [13].

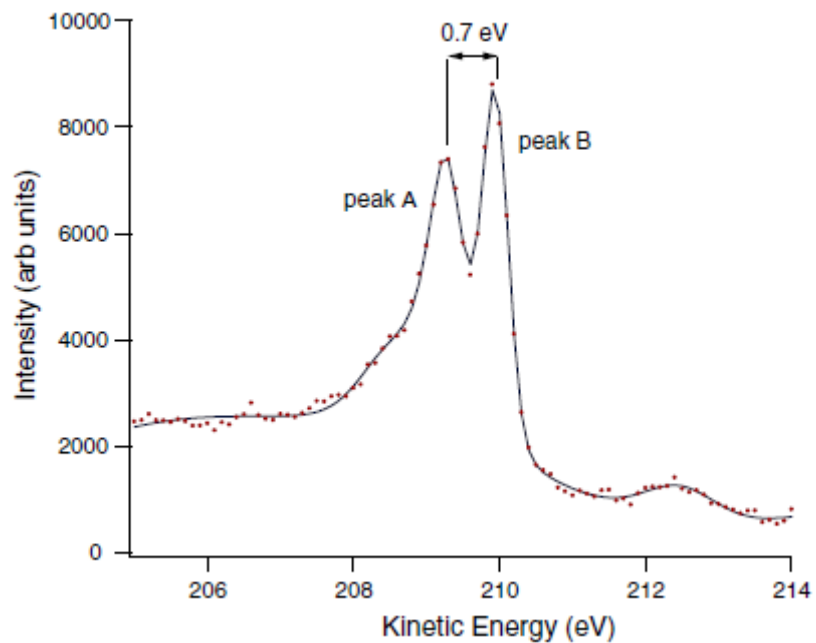


Fig. 2. Typical C 1s photoemission spectrum or EDC from the 0.6 ML $c(\sqrt{3}\times 5)$ rect. phase of CO on Pt(111) showing the two C 1s peaks associated with the two different adsorption sites on the surface. (Photon energy ~ 495 eV.)

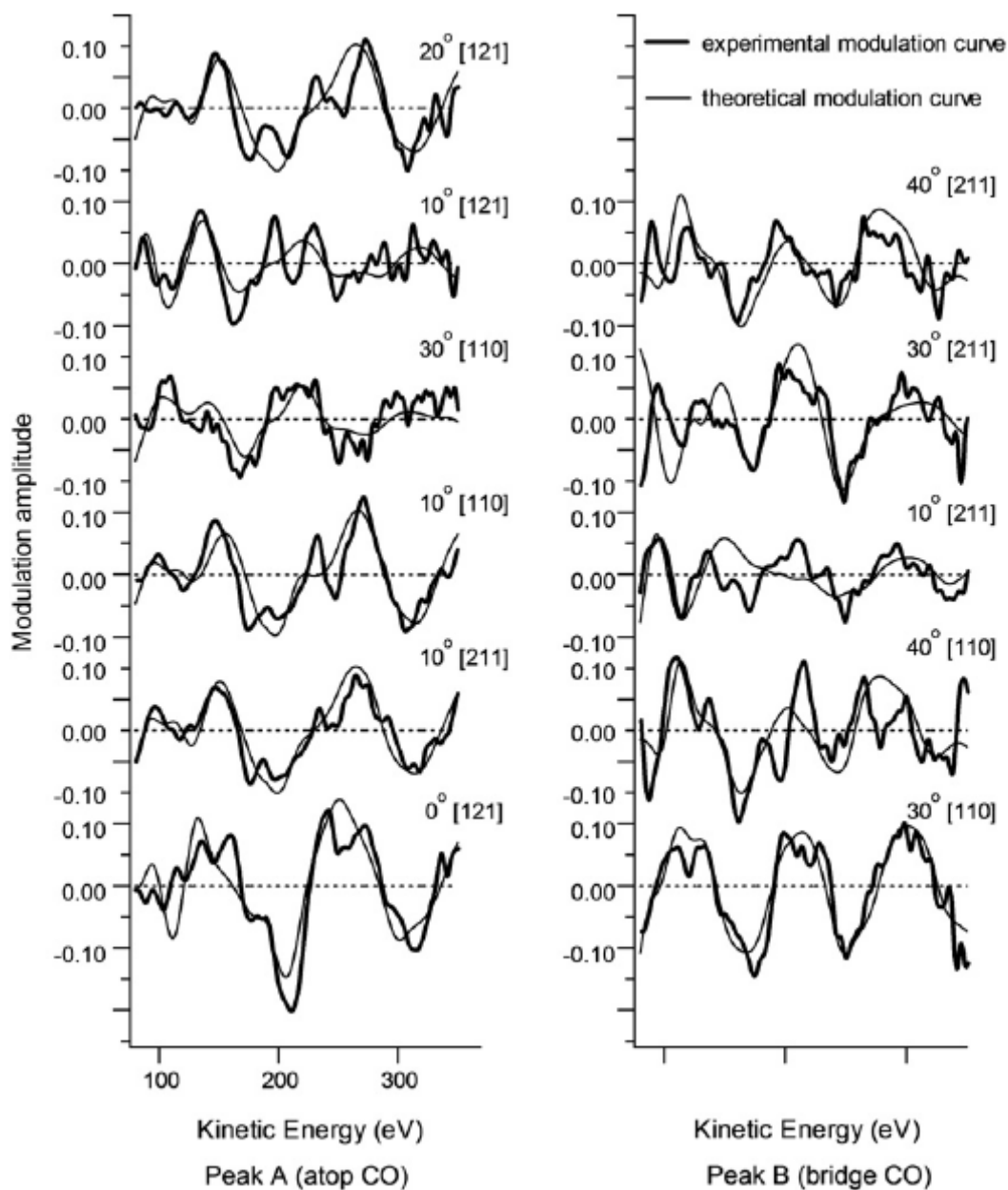


Fig. 3. Comparison of the experimental C 1s modulation curves for different emission angles from the two chemically-shifted component peaks (corresponding to the atop and bridge CO species) with the calculated results for the best fit of model of fig. 4 (a). The spectra are offset for clarity.

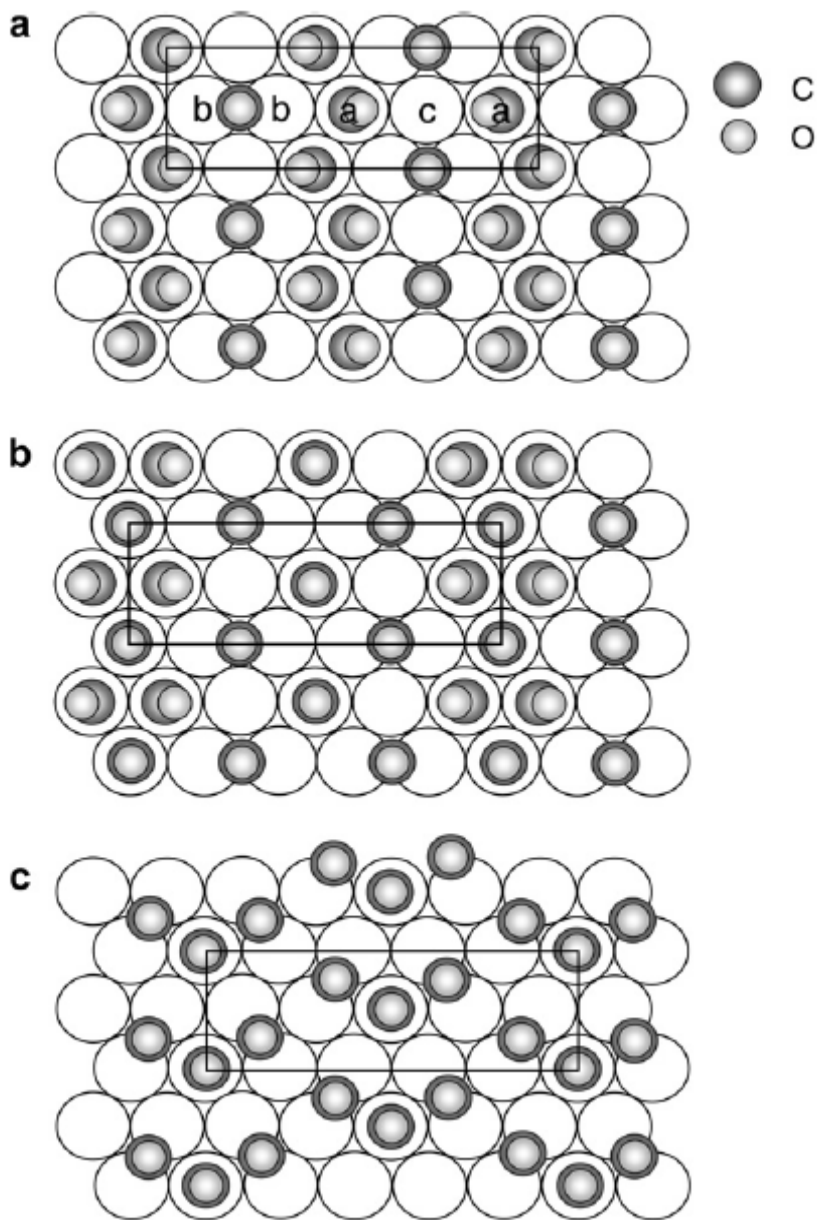


Fig. 4. Alternative models for the $c(\sqrt{3} \times 5)\text{rect.}$ phase of CO on Pt(111) that were considered in this work. (a) is the suggestion of Persson *et al.* [13] as shown in fig. 1. (b) is the model suggested by Avery [6]. (c) is the model suggested by Petrova and Yakovkin [37]. The unit mesh is shown by a rectangle.

References

- [1] G. Ertl, M. Neumann and K.M. Streit, *Surf. Sci.* 64 (1977) 393.
- [2] J.C. Tracey and P.W. Palmberg, *J. Chem. Phys.* 51 (1969) 4852.
- [3] N. Sheppard and N.T. Nguyen, *Adv. IR Raman Spectrosc.* 5 (1978) 67.
- [4] H. Froitzheim, H. Hopster, H. Ibach and S. Lehwald, *Appl. Phys.* 13 (1977) 147.
- [5] A.M. Baró and H. Ibach, *J. Chem. Phys.* 71 (1979) 4812.
- [6] N. Avery, *J. Chem. Phys.* 74 (1981) 4202.
- [7] H. Steininger, S. Lehwald and H. Ibach, *Surf. Sci.* 123 (1982) 264.
- [8] H.-J. Krebs and H. Lüth, *Appl. Phys.* 14 (1977) 337.
- [9] B.E. Hayden and A.M. Bradshaw, *Surf. Sci.* 125 (1983) 787.
- [10] E. Schweizer, B.N.J. Persson, M. Tüschaus, D. Hoge and A.M. Bradshaw, *Surf. Sci.* 213 (1989) 49.
- [11] J.P. Biberian and M.A. Van Hove, *Surf. Sci.* 138 (1984) 361.
- [12] P. Uvdal, P.-A. Karlsson, C. Nyberg, S. Andersson and N.V. Richardson, *Surf. Sci.* 202 (1988) 167.
- [13] B.N.J. Persson, M. Tüschaus and A.M. Bradshaw, *J. Chem. Phys.* 92 (1990) 5034.
- [14] K.-M. Schindler, Ph. Hofmann, K.-U. Weiss, R. Dippel, V. Fritzsche, A. M. Bradshaw, D. P. Woodruff, M.E. Davila, M.C. Asensio, J.C. Conesa and A.R. González-Elipé, *J. Electr. Spectros .Rel. Phenom.* 64/65 (1993) 75.
- [15] M.E. Davila, M.C. Asensio, D.P. Woodruff, K.-M. Schindler, Ph. Hofmann, K.-U. Weiss, R. Dippel, P. Gardner, V. Fritzsche, A.M. Bradshaw, J.C. Conesa and A.R. González-Elipé, *Surf. Sci.* 311 (1994) 337.
- [16] L.D. Mapledoram, M.P. Bessent, A.D. Wander and D.A. King, *Chem. Phys. Lett.* 228 (1994) 527.
- [17] T. Gießel, O. Schaff, C.J. Hirschmugl, V. Fernandez, K.-M. Schindler, A. Theobald, S. Bao, W. Berndt, A.M. Bradshaw, C. Baddeley, A.F. Lee, R.M. Lambert and D.P. Woodruff, *Surf. Sci.* 406 (1998) 90.
- [18] D.F. Ogletree, M.A. Van Hove and G.A. Somorjai, *Surf. Sci.* 173 (1986) 351.
- [19] I. Zsada and M.A. Van Hove, *Surf. Rev. Lett.* 7 (2000) 15.
- [20] M.O. Pederson, M.L. Bocquet, P. Sautet, E. Laegsgaard, I. Stensgaard and F.

-
- Besenbacher, Chem. Phys. Lett. 299 (1999) 403.
- [21] O. Bjorneholm, A. Nilsson, H. Tillborg, P. Bennich, A. Sandell, B. Hernnas, C. Puglia and N. Martensson, Surf. Sci. 315 (1994) L983.
- [22] P.J. Feibelman, B. Hammer, J.K. Nørskov, F. Wagner, M. Scheffler, R. Stumpf, R. Watwe and J. Dumesic, J. Phys. Chem. B 105 (2001) 4018.
- [23] H. Orita, N. Itoh and Y. Inada, Chem Phys. Lett. 384 (2004) 271.
- [24] K. Doll, Surf. Sci. 573 (2004) 464.
- [25] A. Gil, A. Clotet, J.M. Ricart, G. Kresse, M. Garcia-Hernández, N. Rösch and P. Sautet, Surf. Sci. 530 (2003) 71.
- [26] G. Kresse, A. Gil and P. Sautet, Phys. Rev. B 68 (2003) 073401.
- [27] L. Köhler and G. Kresse, Phys. Rev. B 70 (2004) 165405.
- [28] J.A. Steckel, A. Eichler and J. Hafner, Phys. Rev. B 68 (2003) 085416.
- [29] D.P. Woodruff and A.M. Bradshaw, Rep. Prog. Phys. 57 (1994) 1024.
- [30] F. Bondino, G. Comelli, F. Esch, A. Locatelli, A. Baraldi, S. Lizzit, G. Paolucci and R. Rosei, Surf. Sci. Lett. 459 (2000) L467.
- [31] M. Kiskinova, A. Szabo and J.T. Yates, Jr. Surf. Sci. 205 (1988) 215.
- [32] J.S. McEwan, S.H. Payne, H.J. Kreuzer, M. Kinne, R. Denecke and H.P. Steinrück, Surf. Sci. 545 (2003) 47.
- [33] K. J. S. Sawhney, F. Senf, M. Scheer, F. Schäfers, J. Bahrtdt, A. Gaupp and W. Gudat, Nucl. Instrum. Methods A 390 (1997) 395.
- [34] V. Fritzsche, Surf. Sci. 213 (1989) 648.
- [35] V. Fritzsche, J. Phys. Condens. Matter 2 (1990) 1413.
- [36] N.A. Booth, R. Davis, R. Toomes, D.P. Woodruff, C. Hirschmugl, K.-M. Schindler, O. Schaff, V. Fernandez, A. Theobald, Ph. Hofmann, R. Lindsay, T. Giessel, P. Baumgärtel and A. M. Bradshaw, Surf. Sci. 387 (1997) 152.
- [37] N.V. Petrova and I.N. Yakovkin, Surf. Sci. 519 (2002) 90.